JOURNAL OF APPLIED BIOANALYSIS, June. 2024, p. 01-19.
https://doi.org/10.53555/jab.v10.001 (ISSN 2405-710X)
Vol. 10, No. 1

OPEN ACCESS

Box-Behnken Design (BBD) Based Optimization of Mucoadhesive Tablet Loaded Nifedipine: *In-vitro* Release and Stability Studies

Anuj Pathak[1,2], Satish Kumar Sharma[1]*

[1]*Professor & Dean, Glocal School of Pharmacy, Glocal School of Pharmacy, Glocal University, Delhi-Yamunotri Marg (State Highway 57), Mirzapur Pole, Distt - Saharanpur, U.P. - 247121, India*
[2]*Dept of Pharmaceutics, KIET School of Pharmacy, KIET Group of Institutions, Ghaziabad, India. 201206*

Nifedipine, classified as a dihydropyridine subclass within calcium channel blockers, is primarily employed as an antihypertensive and antianginal agent. In the setting of persistent stable angina, the IMAGE trial demonstrated a reduction in angina frequency and an increase in mean exercise duration with Nifedipine. To enhance its bioavailability, particularly through selective absorption in the upper gastrointestinal tract, it is recommended to develop a drug delivery system characterized by its ability to adhere to mucosal surfaces and release medication over an extended period in a sustained manner. In pursuit of this, a mucoadhesive tablet was formulated utilizing chitosan, guar gum, and HPMC as polymers. Mucoadhesion plays a crucial role in the tablet's design, encompassing wetting, adsorption, and interpenetration of polymer chains. The different tablet formulations were assessed for total mucoadhesion time, buoyancy lag time, and the percentage of drug release. The results indicated diverse release kinetics influenced by the integration of different polymers and excipients. Comprehending the behaviors of these polymers greatly improved the precision of drug targeting. Examination of the data revealed a combination of release mechanisms, including erosion, diffusion, and swelling. The study's comprehensive insights contribute valuable information regarding dosage form behavior and the impact of polymers on drug release. Notably, the optimized formulation exhibited superior outcomes, suggesting its potential utility for prolonged drug release in the stomach, thereby improving bioavailability and reducing dosing frequency. The drug release mechanism from the optimized formulation was confirmed as non-Fickian transport through the Higuchi pattern.

Keywords: Box-Behnken Design, Mucoadhesive tablet, Nifedipine, Stability, Antihypertensive, non-Fickian transport.

1. Introduction

Oral administration is the most common and effective method, however, the mucoadhesive system is often used. This mechanism interacts with a mucus layer including epithelial cells and mucin molecules, increasing dose from contact time and improving local and systemic effects. Almost the oral route has the most common and favored by patients due to its ease of use in the mucoadhesive drug delivery system. For several medication categories, the mucoadhesive drug delivery method is the oldest and most effective dosage form (Pankaj et al., 2022).

Mucoadhesion refers to the adherence of a polymer to a biological membrane to deliver the drug to a biological system. Epithelial tissue can be used as the biological membrane. Mucoadhesion refers to the notion of sticky attachment to a mucus layer. Mucoadhesion is a very new and developing medication delivery technique. Adhesive dosage is one way to improve drug delivery for that dosage which has a significant barrier to drug penetration in the mucosa of the oral cavity. The mucosa is also permeable since it is linked to numerous blood sources. With pediatric and elderly patients, this method offers rapid action and high patient compliance. Various mucoadhesive polymers can be used to achieve mucoadhesion. Mucoadhesive polymers are a variety of polymers that enhance adhesion. Diffusion, facture, electrical, and adsorption theories are among the theories used to clarify the notion of mucoadhesion. There is a connection between formulation and mucus membranes. Oral, nasal, ocular, vaginal and gastro, are the routes that are used in mucosal for drug administration (Kumar et al., 2017).

A substance should interchange with mucus that is hydrated with a viscous anionic hydrogel layer in which mucosa is protected, to be bio-adhesive. The mucin is mostly made up of crosslinked flexible glycoprotein chains. Additionally, bio/mucoadhesion procedures can be a helpful technique in drug delivery systems with a variety of benefits including longer residence duration of plea location, protection of drug, enhanced penetration and better availability of the drug (Solanki et al., 2012; Reitsma et al., 1980; Date and Nagarsenker, 2007; Benitex et al., 2021). Adhesion is a normal to next normal cell, it is a cell for unknown material, it is a normal cell to a pathological cell, and it is also adhering to a biological substance are the four forms of bio-adhesion that may be identified in biological systems. The mucoadhesion overcomes first-pass metabolism and is utilized to convey biomolecules like peptides, proteins, and oligonucleotides to specific locations (Pandit et al., 2023). A number of elements, type of mucosal tissue & physiochemical assets of polymeric formulations are the factors that influenced the dosage form's mucoadhesive ability. Controlled release methods were employed in the creation and design of mucoadhesive tablets to achieve sustained release with the help of HPMC and chitosan polymers that help in the enhanced drug release time resulted in better disease treatment (Hirose, 2001; Yin et al., 2016; Lee et al., 2011; Aderibigbe et al., 2017).

2. Materials and methods

2.1. Materials

Nifedipine was acquired from Sigma Aldrich, USA. Ac-Di-Sol, HPMC (https://www.sigmaaldrich.com/IN/en/life-science/sigma-aldrich), Guar gum, Chitosan were issued from the central store department of KSOP, Ghaziabad, whereas analytical grade excipients and reagents were used in all other cases.

Methods

2.2.1. Preparation of mucoadhesive tablet

Compression methods and tableting machines were used to produce the tablets. First, all of the active pharmaceutical ingredients (API) and excipients were screened with a #40 sieve to remove any particles greater than the specified size which could affect the tablets' uniformity. Next, the APIs, the polymers, and the excipients were weighed out, and thoroughly ground together in a mortar and pestle to have a mixture that is uniformly mixed. This sieved blend was further crushed to break down agglomerates by the #40 sieve to get fine particles. Once, the polymers were individually dosed to 200mg per tablet dose, they were mixed in the main powder blend. The end product was achieved by mixing this final blend in a rotatory press that was then automatically driven to press the content inside die-cutting discs which produced tablets.

An experimental design of Box-Behnken was experimented with to optimize the tablet preparation and also to determine the best excipients among those screened. It meant that I should perform 25 experiments, 5 of which were trials. Here, the ultimate amounts of selected excipients were mixed with the key drug-polymer mix to which water was added. The interactions with excipients and process parameters and the effects of their critical quality attributes like hardness, friability, dissolution, etc. were analyzed to select an optimized tablet formulation (Meunier et al., 1995; Ossipov, 2015; Manoel et al., 2020).

2.2.2. Designing Experiments for Formulations Loaded with Drug

Nifedipine mucoadhesive tablet production was modulated by using the RSM and Design Expert software (version 10.0.4, Stat-Ease Incorporation). The capability of RSM to identify, develop, and optimize manufacturing and formulation practices

and processes is highlighted. It is based on the experimental design of Box-Behnken Design (BBD) that allows fitting a polynomial equation to the data of the experiment to have a description of the response/s in terms of all the used independent variables. It was the unique parameters optimized during this study that may have contained items such as nifedipine content, polymer type and concentration, compression force, etc that controlled the characteristics of the tablets. The software helped with modeling to find the levels for these variables that produced the tablet attributes which were optimized within the experimental zone (Hussain et al., 2016; Song et al., 2020).

2.2.3. Characterization of optimized nifedipine mucoadhesive formulation

2.2.3.1. Weight Variation

Twenty tablets were chosen at arbitrarily from each composition and considered separately to inspect for percentage deviation. The percentages listed below the strength variance discrepancy conforming to United States Pharmacopeia was permitted (Akteruzzaman et al., 2012; Hosny et al., 2014).

2.2.3.2. Thickness and Diameter

Twenty tablets were picked arbitrarily from the compositions and their compactness was calculated independently with Vernier calipers. It was stated that the fraction of an inch and cumulative percentage were computed (Zakir et al., 2020; Mallepelli et al., 2017).

2.2.3.2. Hardness

The potential of a dosage form to sustain automated collapse while dealing is indicated by its hardness The tablets' adherence has been resolute using an Essential feature made by Mosanto. It was affirmed in Newton's equations. The composition adherence and stiffness were defined. The mean values were indeed estimated and evaluated in kilograms per square centimeter (Kg/cm2) (Raza et al., 2022; De Abreu Engel et al., 2019).

2.2.3.3. Friability

The friability of the pad was assessed utilizing Roche friability. It is given in interest form (percent). In the friability, a six-gram dosage form (basic weight) was placed. For four minutes or a hundred innovations, the friability was set to twenty-five revolutions per minute. The tablets were cleaned and measured once more (last-minute Weight) (Solanki et al., 2016; Adsul et al., 2018).

% Friability = (Initial weight - Final weight) / Final weight x 100

2.2.3.4. Drug Content

Using a howitzer and pulverize, twenty samples were calculated in powder form. A dose of sixty mg nifedipine was mixed with a hundred ml of aqua. 0.1N hydrochloric acid was infrasound for ten minutes approximately thirty minutes. The solvent was unalloyed buttoned by Whatman filter paper, and the nifedipine information was decisive by allotment of optical density at 235 nm on spectra that were recorded. UV spectra were obtained with two beams (Shimadzu-1800) following appropriate infusion. The information was universally calculated with a formula (Samie et al., 2018).

Content uniformity = Optical density attempt / Optical density accepted x100

2.2.3.5. Drug-Excipient Interaction Study

Infrared spectroscopy is employed to understand the interactions between the active pharmaceutical ingredient and supporting agents in a pharmaceutical formulation. To start the preparation of the KBr pellet for infrared spectroscopy, the film is first dried in a hot air oven at 130°C so all the water molecules can be removed. Here, the disintegration process of potassium bromide powder, drug substance (APAAP), and polymer is done by keeping the whole system in a desiccator to protect it from absorption of moisture. Ingredients are passed through a machine that grinds them into a fine powder supported to have uniformity. Using these two powder mixtures, the mixture is forced into a hydraulic press with great pressure for 7 -8 hours with a 1-minute hold time, which results in transparent pellet samples. The pellets are then loaded in the machine where the IR spectroscopy over the specific wavelengths is conducted to obtain the spectra. The yields record these spectra, and the analysis is performed thereafter to determine if there are any incompatibilities or interactions between drug and excipients. This aims to look for whether the quality of excipients is adequate to formulate the medication without the presence or the shifts of the peaks for the functional groups of the drug as well as that of excipients (Venkatpurwar et al., 2011; Shah et al., 2019).

2.2.3.6. Swelling Study

Individual basis measured tablets (specified as W1) were positioned in a glass chalice were full 200 ml of 0.1 N Hydrochloric acid and fertilized at 37°C1°C. before twenty-four hours, at fairly frequent 1-hour durations, The dosage forms were successfully evacuated against the glass jar, and the glut facial liquid was safely separated with paper (Segale et al., 2020; Mukherjee et al., 2019). The inflamed tablets were again weighed and recorded (W2), and the swelling ratio (SR) was estimated by applying the equation.

SI = W2-W1/W1 X 100

SI -Swelling Index
W1-First Weight
W2-Final Weight

2.2.3.7. *In-vitro* Mucoadhesive Study

On a modified physical balance, the bioadhesive strength of the Nifedipine tablets was measured. The adhesion test was performed on the surface of the stomach membrane. The stomach membrane of the goat was removed immediately after the sacrifice. The membrane was first rinsed in distilled water before being treated in a Tyrode solution. The stomach membrane was then sliced into appropriate-sized pieces and transferred to the laboratory in Tyrode solution, where it was maintained at room temperature (Li et al., 2008; Wang and Zhang, 2012). After that we cut the membrane piece then put the membrane on the surface of the assembly and tightened it with screws. After this, fill the Tyrode solution in a beaker and put the assembly in this beaker. Then on one side of the tablet, we use double side tape and on another side of the tablet we stick the membrane at the top of the apparatus there is one weighing balance, and that weighing balance is stuck to a rod, and on the lower side there is a beaker which is attached to a tablet, first we attached the tablet and takes the initial weight and then lose the rod then we will take the final weight of the tablet, so this is the process mucoadhesive strength, one by one we will check all the force that lies in a mucoadhesive tablet. So, these are the readings that were taken and the mucoadhesive strength was measured (Solanki et al., 2021; Ansari et al., 2022; Solanki et al., 2022; Solanki et al., 2013; Solanki et al., 2021; Solanki et al., 2022).

2.2.3.8. In vitro drug release of mucoadhesive tablet

Release profile modules were performed on tablets from all optimum batches. In-vitro dissociation modules were conducted in the system for dissolution to ascertain acquittal profiles from different compositions**.** The United States pharmacopeia type I Dissolution equipment was used to conduct an in-vitro sustained release module of a Nifedipine mucoadhesive tablet. The entire erection was kept at 37+0.5 C and the warmth at 0.1N Hydrochloric acid solution. All these tablets were kept at 50,75 rpm at the era interval five ml of solution was through a pipette and put in a detachment media for a particular time interruption and drained the definite amount of crisp detachment ratio, after these Processes We will take all the solution in an ambered colored test tube and start the ultraviolet spectroscopy at 236 rpm independently. After this, we will compile the sample and design the dissolution contour (Solanki et al., 2022; Ansari et al., 2022; Solanki, et al., 2022).

The type and amount of polymers used by the matrix significantly depend on their in-vitro drug release through the tablets with prolonged action. Sustained release is often a result of increased matrix density and drug diffusion barrier, which is determined by the polymer ratio. To modify release kinetics, mucopolymers such as Nifedipine tablets can also perform this role. Consequently, the right polymer selection and proportions turn out to be paramount to the desired outcomes of the dosing schedule. In other words, the dosing regimen matched with the release profile.

2.2.3.9. Infra-red spectroscopic analysis (IR)

Initially, we subjected potassium bromide (KBr) powder to a one-hour drying process at 130°C in a hot air oven. Following that, we mixed the dehydrated Nifedipine powder with the dried KBr powder and preserved the mixture in a desiccator to maintain its dryness. Subsequently, the pellet was reconstituted using a hydraulic pump and placed back into the desiccator for storage. Upon placement of the formed pellet into the IR Spectroscopy pellet holder, we executed the spectrum run, recorded the spectra, and proceeded with spectrum identification.

2.2.3.10. Differential scanning calorimetry (DSC) of mucoadhesive tablet

Differential scanning calorimetry investigations were conducted with the aim of identifying potential interactions between the nifedipine and the excipients. This provides us with the necessary data to identify any interactions and monitor changes in the drug's crystallinity. Less than 5 mg of nifedipine was placed inside the punctured metal panel and heated at a rate of 10 °C/min. Liquid nitrogen was used to cool the system, and nitrogen gas served as clean air. The thermal differential analyzer was used to determine the DSC (Solanki et al., 2022; Moorthy et al., 2015).

2.3. Stability Studies of mucoadhesive tablet

The optimized composition was subjected to three eternities of stability testing at 40°C and 75 percent RH. The dosage forms were congested in a brown-flushed closed flask and positioned in the quickened stability box for 90 days at 40°C/75 percent RH. The random selection occurred at a specific time intermission of the aboriginal, alternative, and tertiary eternity. The tablets were tested for various physico-chemical guidelines, including drug concentration and in-vitro drug acquittal (Hirose, 2001; Derakhshandeh et al., 2010; Rathee et al., 2023).

3. Result & Discussion

3.1. Development of a formulation containing drugs and qualitative optimization of the preparation method

Table 1. Results from experimental trials conducted using the Box-Behnken Design

Run	*Factor 1* A: HPMC K4M (mg)	*Factor 2* B: HPMC K100M (mg)	*Factor 3* C: Chitosan (mg)	*Factor 4* D: Guar Gum (mg)	*Response 1* Hardness (kg/cm2)	*Response 2* Friability (%)	*Response 3* Thickness (mm)
1	20	40	30	20	5.2	0.46	2.92
2	50	50	30	25	7.1	0.56	3.12
3	20	40	40	25	5.3	0.47	2.93
4	35	50	20	25	5.9	0.51	3.02
5	35	40	20	30	6.1	0.49	2.94
6	35	50	40	25	6.1	0.51	3.04
7	35	40	40	30	6.2	0.5	3.01
8	35	40	30	25	6.1	0.5	3.02
9	20	30	30	25	5.3	0.47	2.96
10	20	50	30	25	5.4	0.46	2.94
11	50	40	30	20	6.5	0.55	3.11
12	35	30	30	30	6.2	0.51	3.12
13	50	40	40	25	6.8	0.55	3.13
14	35	30	20	25	5.6	0.5	3.02
15	50	30	30	25	6.8	0.57	3.12
16	50	40	20	25	6.9	0.56	3.11
17	35	30	40	25	5.9	0.51	3.02
18	35	30	30	20	6.1	0.52	3.05
19	20	40	20	25	5.3	0.48	2.95
20	35	50	30	30	5.9	0.53	2.98
21	35	40	40	20	6	0.54	2.99
22	35	40	20	20	6.2	0.51	3.01
23	50	40	30	30	7	0.57	3.11
24	20	40	30	30	5.4	0.45	2.95
25	35	50	30	20	5.9	0.51	3.02

3.2. Experimental design: model fitting and optimization of parameters

After formulation development the model fitting was done with the help of Design Exert software DX11 (State Ease Incorporation). Response surface methodology was employed and quality by design approach was utilized. The results were found to be in the range of 5.2-7.1, 0.45-0.57 and 2.92-3.13 for hardness, friability and thickness, respectively (Table 1). The predicted R square values were in the arrangement with the adjusted R square value (table 2). 3-D response surface analysis was done to determine the effect of various factors on the response as given in the Figs. 1, 2 and 3.

RSM plays a key role in getting good quality over different segments. RSM, which strategically manipulates multiple factors at the same time, eventually unearths the best conditions for attaining the desired results. It makes it possible to make adjustments in the processes that result in efficiency, yield, and quality maximization and cost reduction. Through the strategic choice of independent variables and experimented one can reveal complex relations between inputs and outputs. This comprehension gives the way to the practitioners to go through the process optimization filter confidently, promoting unceasing improvement and innovation. RSM's flexibility and accuracy are invaluable in the wake of progress in the field of quality control across industries, which in turn, presents opportunities for development and improvement.

Table 2. ANOVA for Linear model: Hardness

Source	*Sum of Squares*	*df*	*Mean Square*	*F-value*	*p-value*	
Model	7.14	4	1.79	66.04	< 0.0001	significant
A-HPMC K4M	7.05	1	7.05	260.88	< 0.0001	
B-HPMC K100M	0.0133	1	0.0133	0.4932	0.4906	
C-Chitosan	0.0075	1	0.0075	0.2774	0.6042	
D-Guar Gum	0.0675	1	0.0675	2.50	0.1298	

Residual	0.5407	20	0.0270
Cor Total	7.68	24	

Factor coding has been encoded, and the sum of squares has been categorized as Type III - Partial. The Model F-value, registering at 66.04, signifies the model's significance. The probability of obtaining an F-value of this magnitude purely by chance is only 0.01%.

Model terms achieve significance when their p-values fall below 0.0500. In this specific analysis, the model term A is considered significant. Conversely, p-values surpassing 0.1000 indicate a lack of significance for the corresponding model terms. If a considerable number of model terms are deemed insignificant (excluding those essential for maintaining hierarchy), reducing the model size may improve overall performance.

Table 3. Fit Statistics

Std. Dev.	**0.1644**	**R^2**	**0.9296**
Mean	6.05	**Adjusted R^2**	0.9155
C.V. %	2.72	**Predicted R^2**	0.8883
		Adeq Precision	22.8917

The **anticipated R^2** value of 0.8883 aligns reasonably with the **Adjusted R^2** of 0.9155, indicating a difference of less than 0.2.

Adeq Precision evaluates the signal-to-noise ratio, with a preference for a ratio exceeding 4. Your ratio of 22.892 signifies a satisfactory signal level. Consequently, this model proves effective for exploring the design space.

Hardness = + 6.05 + 0.7667A + 0.0333B + 0.0250C + 0.0750D

Table 4. Run Order Analysis: Actual vs Predicted Values, Residuals, and Leverage

Run Order	*Actual Value*	*Predicted Value*	*Residual*	*Leverage*
1	5.20	5.21	-0.0063	0.207
2	7.10	6.85	0.2520	0.207
3	5.30	5.31	-0.0063	0.207
4	5.90	6.06	-0.1563	0.207
5	6.10	6.10	0.0020	0.207
6	6.10	6.11	-0.0063	0.207
7	6.20	6.15	0.0520	0.207
8	6.10	6.05	0.0520	0.040
9	5.30	5.25	0.0520	0.207
10	5.40	5.31	0.0853	0.207
11	6.50	6.74	-0.2397	0.207
12	6.20	6.09	0.1103	0.207
13	6.80	6.84	-0.0397	0.207
14	5.60	5.99	-0.3897	0.207
15	6.80	6.78	0.0187	0.207
16	6.90	6.79	0.1103	0.207
17	5.90	6.04	-0.1397	0.207
18	6.10	5.94	0.1603	0.207
19	5.30	5.26	0.0437	0.207
20	5.90	6.16	-0.2563	0.207
21	6.00	6.00	0.0020	0.207
22	6.20	5.95	0.2520	0.207
23	7.00	6.89	0.1103	0.207
24	5.40	5.36	0.0437	0.207
25	5.90	6.01	-0.1063	0.207

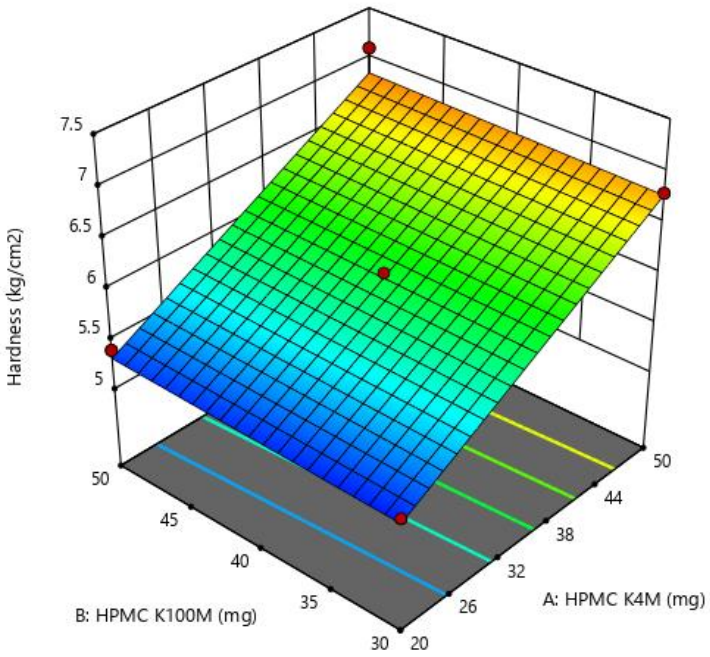

Fig. 1. 3D response surface plot representing the effect of factors on the hardness

Table 5. ANOVA for Linear model of Friability

Source	*Sum of Squares*	*df*	*Mean Square*	*F-value*	*p-value*	
Model	0.0273	4	0.0068	47.82	< 0.0001	Significant
A-HPMC K4M	0.0271	1	0.0271	189.82	< 0.0001	
B-HPMC K100M	0.0000	1	0.0000	0.0000	1.0000	
C-Chitosan	0.0001	1	0.0001	0.5258	0.4768	
D-Guar Gum	0.0001	1	0.0001	0.9348	0.3452	
Residual	0.0029	20	0.0001			
Cor Total	0.0301	24				

Factor coding has been successfully completed, and the categorization of the sum of squares has been achieved using a Type III - Partial approach. The Model F-value, recorded at 47.82, indicates the model's significance. The probability of such a substantial F-value occurring by random chance is only 0.01%.

Model terms are deemed significant if their p-values are below 0.0500. In this case, A emerges as a noteworthy model term. Conversely, model terms with values surpassing 0.1000 are considered not significant. If there are multiple insignificant model terms (excluding those essential for hierarchy), optimizing the model by reducing such terms could potentially enhance its performance.

Table 6. Fit Statistics

Std. Dev.	**0.0119**	**R^2**	**0.9053**
Mean	0.5116	**Adjusted R^2**	0.8864
C.V. %	2.33	**Predicted R^2**	0.8518
		Adeq Precision	19.0350

The expected R^2 value of 0.8518 is in reasonable agreement with the Adjusted R^2 of 0.8864, suggesting a difference of less than 0.2.

Adeq Precision assesses the signal to noise ratio, and a ratio exceeding 4 is preferred. With a ratio of 19.035, the signal level is deemed satisfactory. As a result, this model is suitable for exploring the design space.

Friability = + 0.5116 + 0.0475A + 0.0000B + 0.0025C - 0.0033D

Table 7. Report on Discrepancies Between Actual and Predicted Data

Run Order	*Actual Value*	*Predicted Value*	*Residual*	*Leverage*
1	0.4600	0.4674	-0.0074	0.207
2	0.5600	0.5591	0.0009	0.207
3	0.4700	0.4666	0.0034	0.207
4	0.5100	0.5091	0.0009	0.207
5	0.4900	0.5058	-0.0158	0.207
6	0.5100	0.5141	-0.0041	0.207
7	0.5000	0.5108	-0.0108	0.207
8	0.5000	0.5116	-0.0116	0.040
9	0.4700	0.4641	0.0059	0.207
10	0.4600	0.4641	-0.0041	0.207
11	0.5500	0.5624	-0.0124	0.207
12	0.5100	0.5083	0.0017	0.207
13	0.5500	0.5616	-0.0116	0.207
14	0.5000	0.5091	-0.0091	0.207
15	0.5700	0.5591	0.0109	0.207
16	0.5600	0.5566	0.0034	0.207
17	0.5100	0.5141	-0.0041	0.207
18	0.5200	0.5149	0.0051	0.207
19	0.4800	0.4616	0.0184	0.207
20	0.5300	0.5083	0.0217	0.207
21	0.5400	0.5174	0.0226	0.207
22	0.5100	0.5124	-0.0024	0.207
23	0.5700	0.5558	0.0142	0.207
24	0.4500	0.4608	-0.0108	0.207
25	0.5100	0.5149	-0.0049	0.207

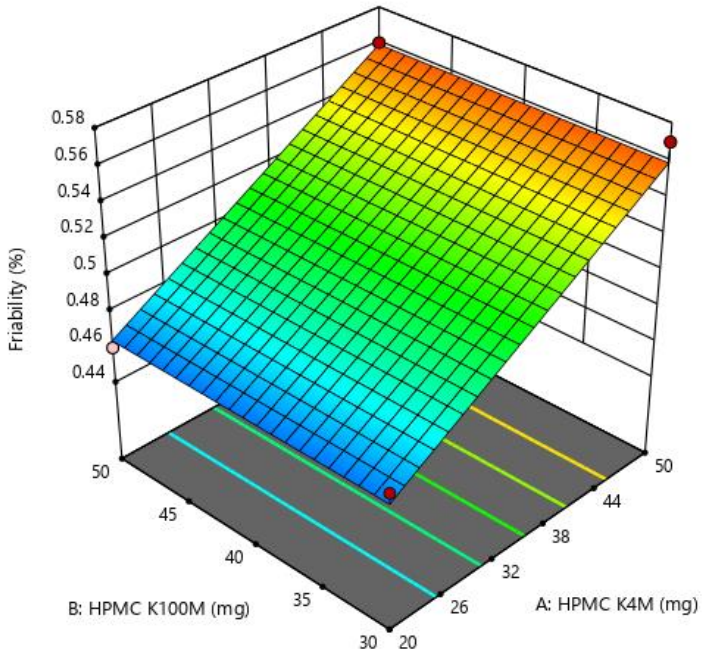

Fig. 2. Creating a 3D Surface Plot to Illustrate the Impact of Variables on Friability

Table 8. ANOVA for Linear Model Thickness

Source	*Sum of Squares*	*df*	*Mean Square*	*F-value*	*p-value*	
Model	0.0947	4	0.0237	24.06	< 0.0001	significant
A-HPMC K4M	0.0919	1	0.0919	93.39	< 0.0001	
B-HPMC K100M	0.0024	1	0.0024	2.45	0.1334	
C-Chitosan	0.0004	1	0.0004	0.4151	0.5267	
D-Guar Gum	8.333E-06	1	8.333E-06	0.0085	0.9276	
Residual	0.0197	20	0.0010			
Cor Total	0.1144	24				

The coding of factors has been completed. The sum of squares follows a Type III - Partial approach.

The Model F-value, which stands at 24.06, signifies the significance of the model. The likelihood of such a large F-value occurring solely due to random noise is merely 0.01%.

Identify the importance of model terms based on their p-values; those with values below 0.0500 are deemed significant, with A standing out in this context. On the contrary, model terms surpassing 0.1000 are considered non-significant. If insignificant model terms are abundant (excluding those vital for hierarchy), optimizing the model by minimizing such terms may improve its overall performance.

Table 9. Statistical Summary and Model Evaluation Metrics

Std. Dev.	**0.0314**	**R^2**	**0.8280**
Mean	3.02	**Adjusted R^2**	0.7936
C.V. %	1.04	**Predicted R^2**	0.7267
		Adeq Precision	14.4957

The anticipated R^2 of 0.7267 aligns reasonably with the Adjusted R^2 of 0.7936, indicating a difference of less than 0.2.

Adeq Precision evaluates the signal-to-noise ratio with a preference for a ratio greater than 4 is desirable. Your ratio of 14.496 signifies a satisfactory signal level. Consequently, This model can be applicable to explore the design space.

Thickness = + 3.02 + 0.0875A - 0.0142B + 0.0058C + 0.0008D

Table 10. Report on Discrepancies Between Actual and Predicted Data

Run Order	*Actual Value*	*Predicted Value*	*Residual*	*Leverage*
1	2.92	2.94	-0.0153	0.207
2	3.12	3.10	0.0231	0.207
3	2.93	2.94	-0.0119	0.207
4	3.02	3.00	0.0164	0.207
5	2.94	3.02	-0.0786	0.207
6	3.04	3.02	0.0247	0.207
7	3.01	3.03	-0.0203	0.207
8	3.02	3.02	-0.0036	0.040
9	2.96	2.95	0.0097	0.207
10	2.94	2.92	0.0181	0.207
11	3.11	3.11	-0.0003	0.207
12	3.12	3.04	0.0814	0.207
13	3.13	3.12	0.0131	0.207
14	3.02	3.03	-0.0119	0.207
15	3.12	3.13	-0.0053	0.207
16	3.11	3.11	0.0047	0.207
17	3.02	3.04	-0.0236	0.207
18	3.05	3.04	0.0131	0.207
19	2.95	2.93	0.0197	0.207
20	2.98	3.01	-0.0303	0.207
21	2.99	3.03	-0.0386	0.207
22	3.01	3.02	-0.0069	0.207
23	3.11	3.11	-0.0019	0.207
24	2.95	2.94	0.0131	0.207
25	3.02	3.01	0.0114	0.207

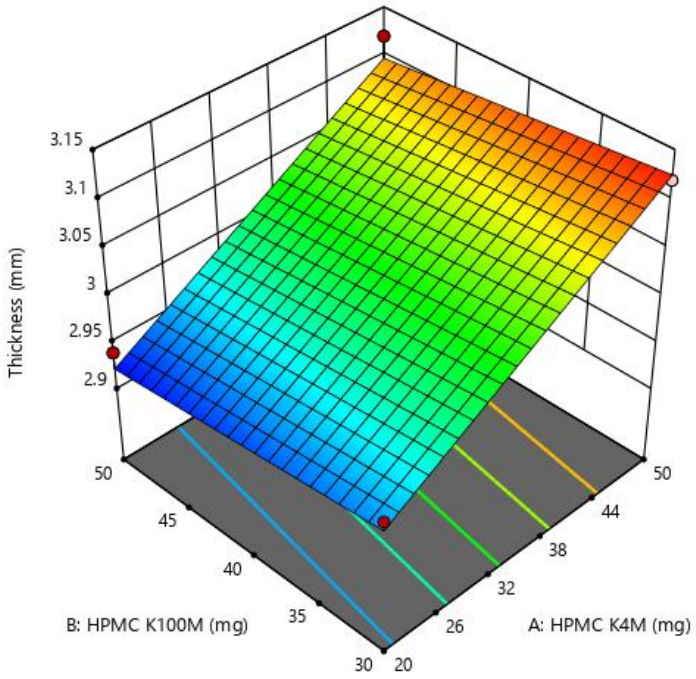

Fig. 3. Creating a 3D Surface Plot to Illustrate the Impact of Variables on Thickness

3.3. Analysis of Desirability

The Figures above reveal that the desirability of the optimized system surpasses 0.78, indicating its appropriateness for selection. The decision-making process will rely on the information shown in Fig. 4.

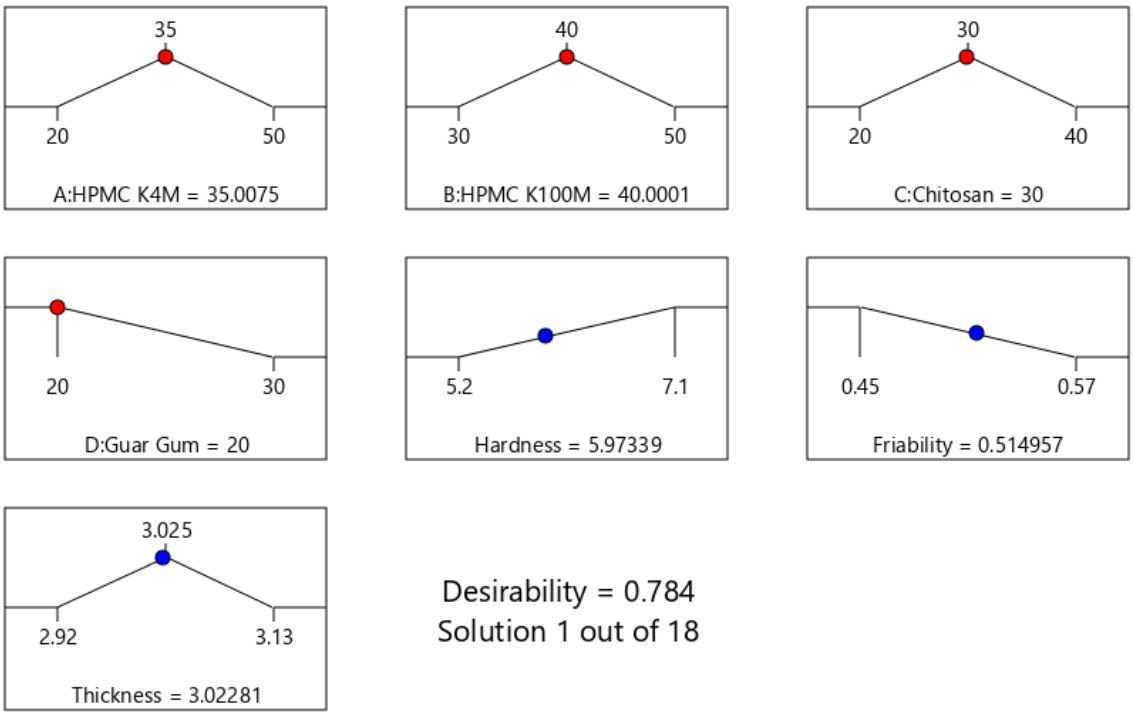

Fig. 4. Desirability of different optimization parameters of factors and response

3.4. Confirmation of location and data suitability

Following the utilization of numerical and graphical optimization instruments, the analysis revealed that optimal outcomes can be achieved by adhering to the specified concentration levels of factors outlined in Table 8. The conclusive results will be documented in Table 9.

Table 11. Confirmation Location (Optimized formulation)

HPMC K4M	*HPMC K100M*	*Chitosan*	*Guar Gum*
35.0002	40	30	20.0001

Table 12. Results Obtained of final optimized formulation

Hardness	*Friability*	*Thickness*
5.9	0.51	3.02
6	0.52	3.01
5.9	0.51	3.02

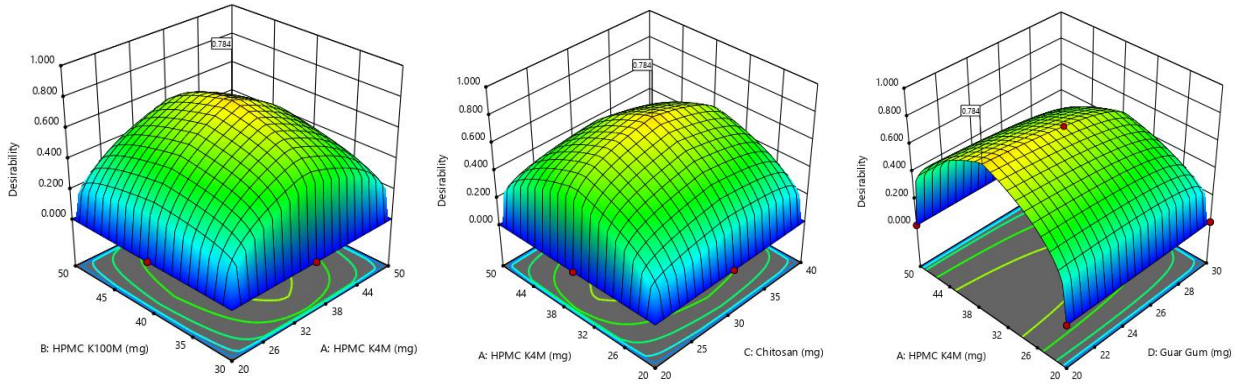

Fig. 5. Plotting the Desirability of an Optimized System

3.5. Analysis of Overlay plot

The overlay graph indicates that the parameters, which have been developed and optimized, are seamlessly aligned within the system's boundaries. This suggests their suitability for assessing the data, as illustrated in Fig. 6.

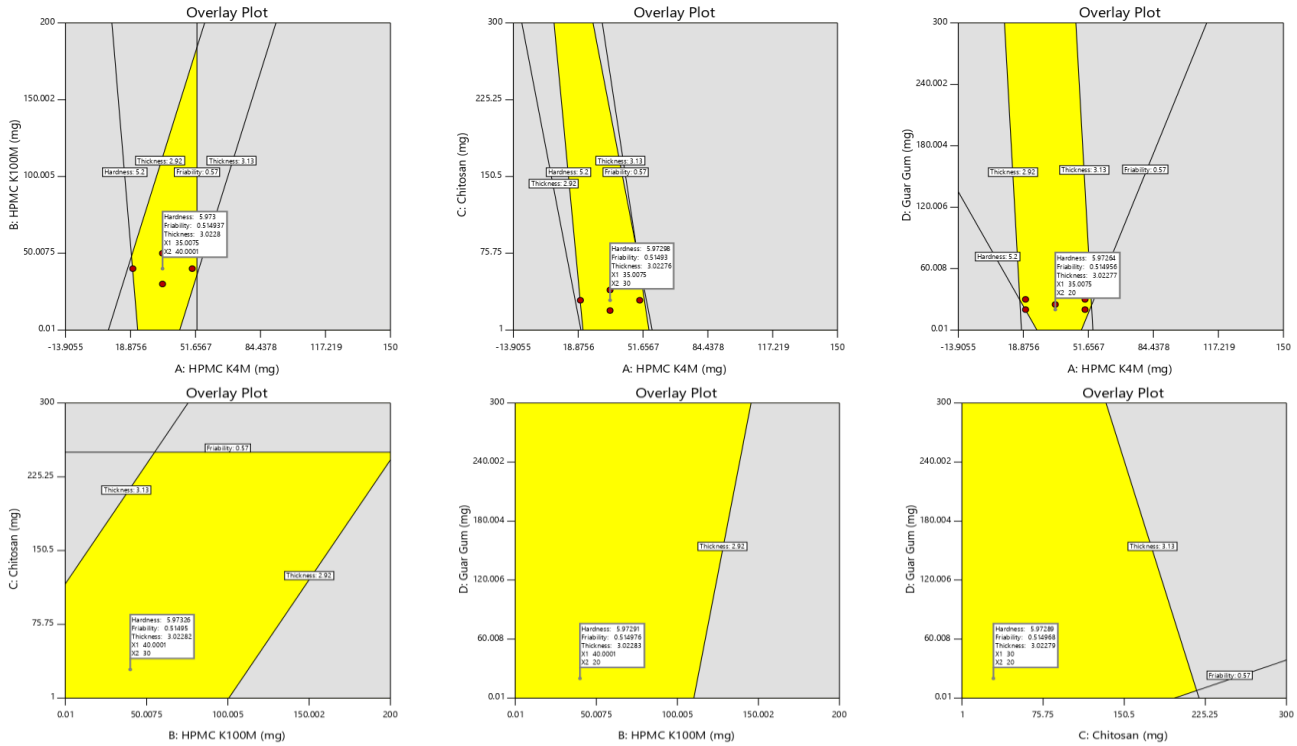

Fig. 6. Overlay plot of all the factors and responses

3.6. Swelling study

The swelling index was computed as a function of time. As the tablet's weight gain enhanced proportionally to the rate of hydration, the swelling index increased significantly. The swelling index of an optimized formulation containing Carbopol 934P in a concentration of 25% achieved a considerable swelling of 187.10% in 6 hrs for other polymers.

The swelling index of the optimized formulation emphasizes the key role of polymers in tablet

swelling. The variation of polymer type influences the swelling behavior enormously, while hydrophilic polymers such as HPMC tend to swell more than hydrophobic polymers. The type-of-polymer selection, consequently, determines tablet properties such as the kinetics of drug release and overall performance.

3.7. Drug Release Patterns from Mucoadhesive Nifedipine Tablets in an In-Vitro Setting

The objective of conducting in-vitro dissolution testing was to assess the potential of the polymer in mucoadhesive gastro retentive drug delivery, ensuring sustained release and extended gastric retention time. The dissolution tests were performed on all batches over 8 hours, and the outcomes are depicted in Fig. 9. It was observed that the release of Nifedipine from mucoadhesive tablets varied based on the polymer ratio and type. Analyzing the data, it was found that the optimized formulation, incorporating Carbopol 934, exhibited a reduced rate of swelling, minimal erosion, superior mucoadhesion, and achieved a release of 94.62%. These findings align with the desired criteria for drug release within the specified lag time of 8 hours.

The swelling behavior is an important element of mucoadhesive formulation assessment and it is important to know what it means. Swelling indicates the extent of association with the mucosal surfaces thus, the formation of a gel layer occurs, which changes drug release and bioavailability. In the case of drug delivery in the gastrointestinal tract, maintaining optimal swelling (by adjusting the ionic charges and the polymers) is very crucial. This eventually results in increased residence time, thereby enhancing adhesion and therapeutic outcomes in mucosal drug delivery applications.

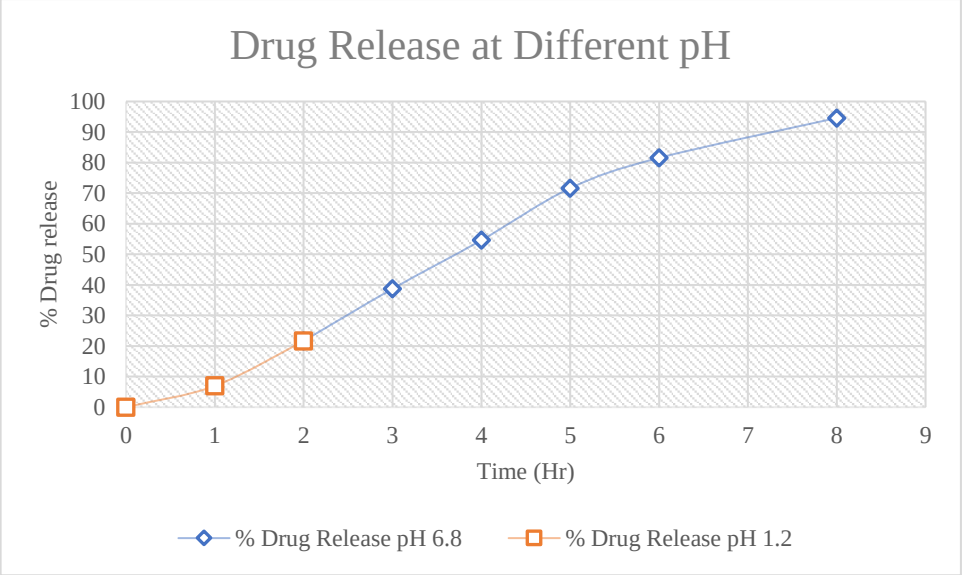

Fig. 7. Variations in pH Impacting the Release Profile of Press-Coated Tablet Medications

3.8. Infra-red spectroscopic analysis

FT-IR Spectroscopy was employed to identify the drug, and various peaks corresponding to different functional groups were detected. These observed peaks closely resembled the standard values provided in the USP/IP[42]. The spectrum depicted in Fig. 10 displayed distinct peaks corresponding to various functional groups. The FTIR analysis indicated the absence of any interactions, confirming that all the excipients exhibited a non-interactive nature (Solanki et al., 2021; Tiwari et al., 2021; Elian and Hackett, 2015; Faria, 2020).

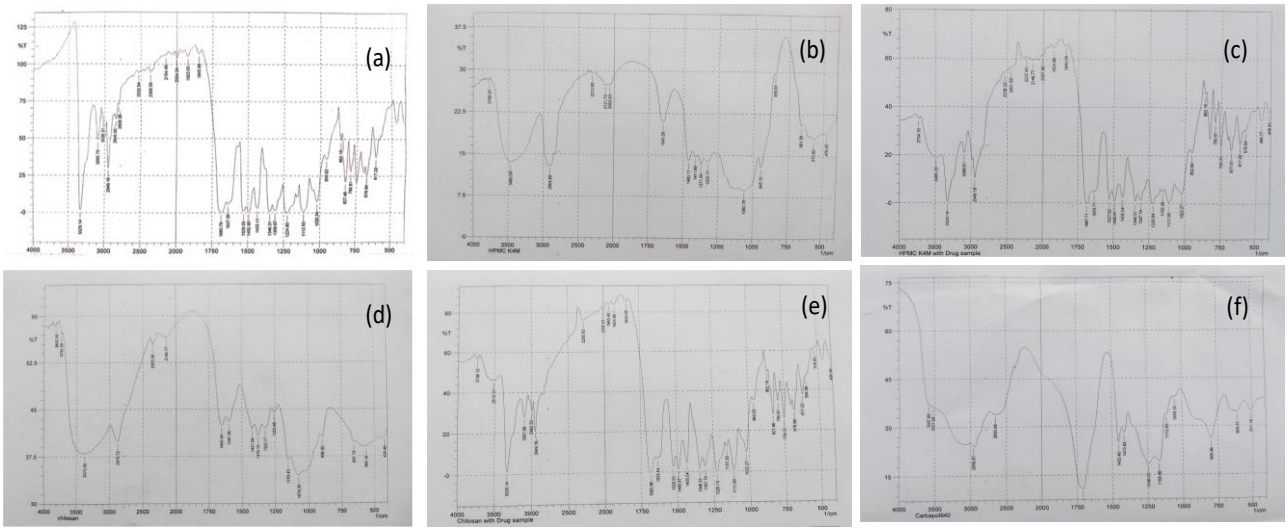

Fig. 8. FTIR analysis of (a) Nifedipine, (b) HPMC K4M, (c) Mixture of Nifedipine and HPMC, (d) Chitosan, (e) Chitosan with Nifedipine and (f) Carbopol with Nifedipine

Polymer Carbopol 934P was selected in the first place as that is the most powerful mucoadhesive agent, as it is known to be less prone to rapid swelling and erosion. Thus it provides a prolonged nifedipine release that lasts for 8 hours. Compatibility was the aspect that could be seen from the fact that there was no interaction of nifedipine and carbopol when they were examined in FTIR.

3.9. Differential scanning calorimetry (DSC)

DSC experiments were conducted to evaluate the crystallinity and impurities of the drug by examining its melting point. The polymorphic nature of Nifedipine resulted in a single exothermic peak at 174.5°C in the DSC thermogram. Notably, the exothermic peak observed at 174.5°C for Nifedipine exhibited a slight shift to 174.6°C, indicating the absence of molecular interactions between Nifedipine and the HPMC matrix during the formulation development process (refer to Fig. 11).

Furthermore, one definitive melting endotherm that is important is that the formulation that contains nifedipine remains in its pure crystalline state. Maintaining crystallinity is an important factor because it prevents drug dissolution as well as the possibility of amorphous forms being more chemically reactive than crystalline ones. Overall, it's clear that the minuscule fluctuation possessed by the nifedipine melting point in HPC matrices is a convincing sign that the medication itself is chemically and physically stable. The stability data is also one more reason to select HPMC as a likely candidate excipient which will not affect the shelf life or bioavailability of nifedipine by excipient's impact. Tracking crystallization behavior using scanning microcalorimetry in a fast manner will enable the detection of any growing changes in the molecular stability to ensure product quality is preserved until the end of the shelf period.

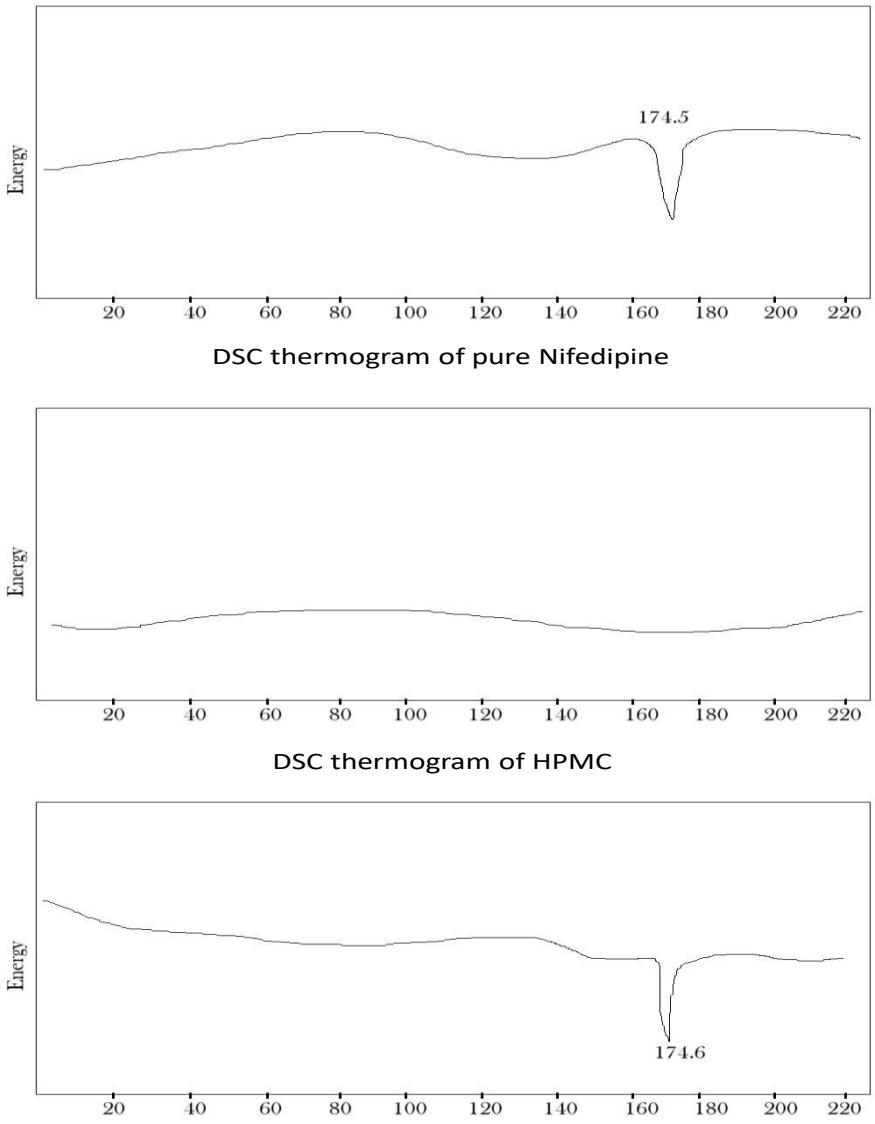

Fig. 9. DSC Thermogram of pure Nifedipine, HMPC and its mixture

3.10 . Storage stability Assessment of optimized formulation

The concept of stability refers to the duration during which a drug maintains its original properties as established during the manufacturing process. To assess stability, the optimized formulation underwent testing in accordance with guidelines outlined by the U.S. FDA and ICH. The formulation underwent exposure to varied temperatures, specifically 25°C/60% RH, 30°C/65% RH, and 40°C/7%, over durations of 15, 30, and 45 days. Periodic analysis of the stored samples was conducted to monitor alterations in physical properties, hardness, drug content, and compatibility.

The findings indicated that the optimized formulation exhibited commendable stability, with no discernible significant changes observed in the tablets after storage under diverse conditions.

Table 13. Investigation of Stability Studies performed on optimized formulation

Time period (Days)	*% Drug release*	*Drug content*	*Mucoadhesive strength*
0	98.91	99.18	38.79
30	98.86	99.10	38.72
60	98.74	99.07	38.66
90	98.68	98.33	38.61
180	98.05	98.21	38.55

The optimization data demonstrate the formulated product has stable attributes under ordinary temperature and moisture conditions for the expected duration in the market. This will serve as a guarantee that the product is still potent when it is kept on store shelves by suppliers, retail outlets, and patients. Sticking to ICH and FDA stability assessment guidelines not only shows compliance with the regulatory authorities regarding efficacy and safety but also helps the product sail through the approval process and stay in the market. Collectively these favorable stability results assure the formulation quality and predictability after construction and scale up.

4. Conclusion

The FTIR examination reveals the absence of any interaction between the drug and the polymer employed in the research. The mucoadhesive property of Nifedipine tablets containing variable quantity of polymers was resolute with an assessment to advance a good adhesiveness deprived of any difficulties. The type and concentration of bioadhesive polymers influenced the bioadhesion characteristics. The highest mucoadhesion force was proposed by optimized formulation comprising Carbopol 934P. It was observed that the release of Nifedipine from mucoadhesive tablets varied according to the ratio and type of polymer. From the above data, an optimized formulation containing Carbopol 934 showed a lesser rate of swelling, less erosion, and better mucoadhesion, and released 94.78% which shows the desired criteria for the release of the drug within the required lag time of 8 hrs. Higuchi's equation best describes optimal formulation for drug release mechanisms, exhibiting anomalous behavior in the formulations.

References

1. Aderibigbe, B., Aderibigbe, I., & Popoola, P. (2017). Design and biological evaluation of delivery systems containing bisphosphonates. Pharmaceutics, 9(1), 1–24. https://doi.org/10.3390/pharmaceutics9010002
2. Adsul, S., Bidkar, J. S., Harer, S., & Dama, G. Y. (2018). RP-HPLC Method Development and Validation for Simultaneous Estimation for Metformin and Sitagliptin in Bulk and Tablet Formulation. International Journal of ChemTech Research, 11(11). https://doi.org/10.20902/ijctr.2018.111149.
3. Akteruzzaman, M., Rahman, A., Sultan, M. Z., Islam, F., Salam, M. A., & Rashid, M. A. (2012). Development and validation of a simple RP-HPLC method for simultaneous estimation of metformin hydrochloride and rosiglitazone in pharmaceutical dosage forms. Dhaka University Journal of Pharmaceutical Sciences, 11(2). https://doi.org/10.3329/dujps.v11i2.14574
4. Ansari, M. D., Khan, I., Solanki, P., Pandit, J., Jahan, R. N., Aqil, M., & Sultana, Y. (2022). Fabrication and Optimization of Raloxifene Loaded Spanlastics Vesicle for Transdermal Delivery. Journal of Drug Delivery Science and Technology, 68(January), 103102. https://doi.org/10.1016/j.jddst.2022.103102.
5. Ansari, M. D., Saifi, Z., Pandit, J., Khan, I., Solanki, P., Sultana, Y., & Aqil, M. (2022). Spanlastics: A novel nanovesicular carrier - Its potential application and emerging trends in therapeutic delivery. AAPS PharmSciTech, 23(4). https://doi.org/10.1208/s12249-022-02217-9.
6. Benitex, Y., Davis, J., Wensel, D. L., Mitchell, T. S., Krystal, M. R., & Drexler, D. M. (2021). Utility of LC-MS Surrogate Peptide Methodology in the Development of a Combinectin, a Unique Anti-HIV Biologic Drug. Journal of Applied Bioanalysis, 7(3), e21007–e21007. https://doi.org/10.17145/jab.21.007
7. Date, A. A., & Nagarsenker, M. S. (2007). Design and evaluation of self-nanoemulsifying drug delivery systems (SNEDDS) for cefpodoxime proxetil. International Journal of Pharmaceutics, 329(1–2), 166–172. https://doi.org/10.1016/j.ijpharm.2006.08.038
8. De Abreu Engel, R. E., Thomas Barden, A., Chagas Campanharo, S., Olegário, N., Volpato, N. M., & Scherman Schapoval, E. E. (2019). Evaluation of linagliptin dissolution from tablets using HPLC and UV methods. Drug Analytical Research, 3(2). https://doi.org/10.22456/2527-2616.97847
9. Derakhshandeh, K., Soheili, M., Dadashzadeh, S., & Saghiri, R. (2010). Preparation and in vitro characterization of 9-nitrocamptothecin-loaded long circulating nanoparticles for delivery in cancer patients. International Journal of Nanomedicine, 5(1). https://doi.org/10.2147/ijn.s11586.
10. Elian, A. A., & Hackett, J. (2015, July 15). Urine analysis of buprenorphine/norbuprenorphine/naloxone in drugs and driving cases. Journal of Applied Bioanalysis, 1(3), 80–88. https://doi.org/10.17145/jab.15.014
11. Faria, M. (2020, January 15). Addressing Bioanalytical Needs of Antibody-Based Biotherapeutics by LC-MS. Journal of Applied Bioanalysis, 6(1), 7–11. https://doi.org/10.17145/jab.20.003
12. Hirose, K. (2001). A practical guide for the determination of binding constants. Journal of Inclusion Phenomena, 39(3–4), 193–209. https://doi.org/10.1023/A:1011117412693
13. Hirose, K. (2001). A Practical Guide for the Determination of Binding Constants. Journal of

Inclusion Phenomena, 39(3–4), 193–209. https://doi.org/10.1023/A:1011117412693.
14. Hosny, K. M., & Aljaeid, B. M. (2014). Sildenafil citrate as oral solid lipid nanoparticles: A novel formula with higher bioavailability and sustained action for treatment of erectile dysfunction. Expert Opinion on Drug Delivery, 11(7), 1015–1022. https://doi.org/10.1517/17425247.2014.912212
15. Hussain, S., Shaikh, T., & Farooqui, M. (2016). Development and validation of liquid chromatography method for the determination and quantification of impurities in imiquimod. British Journal of Pharmaceutical Research, 13(1). https://doi.org/10.9734/bjpr/2016/28020
16. Kumar, P., Sharma, G., Kumar, R., Malik, R., Singh, B., Katare, O. P., & Raza, K. (2017). Enhanced brain delivery of dimethyl fumarate employing tocopherol-acetate-based nanolipidic carriers: Evidence from pharmacokinetic, biodistribution, and cellular uptake studies. ACS Chemical Neuroscience, 8(4), 860–865. https://doi.org/10.1021/acschemneuro.6b00428
17. Lee, S., Glendenning, P., & Inderjeeth, C. A. (2011). Efficacy, side effects and route of administration are more important than frequency of dosing of anti-osteoporosis treatments in determining patient adherence: A critical review of published articles from 1970 to 2009. Osteoporosis International, 22(3), 741–753. https://doi.org/10.1007/s00198-010-1335-x
18. Li, P., Dai, Y. N., Zhang, J. P., Wang, A. Q., & Wei, Q. (2008). Chitosan-Alginate Nanoparticles as a Novel Drug Delivery System for Nifedipine. International Journal of Biomedical Sciences, 4(3).
19. Mallepelli, S., Rao, N., & Nune, S. (2017). Development of a simple, rapid and specific RP-HPLC method for the estimation of metformin and sitagliptin in bulk and combined pharmaceutical dosage forms. International Journal of Pharmaceutical and Biological Sciences, 7(4).
20. Manoel, J. W., Primieri, G. B., Bueno, L. M., Wingert, N. R., Volpato, N. M., Garcia, C. V., Scherman Schapoval, E. E., & Steppe, M. (2020). The application of quality by design in the development of the liquid chromatography method to determine empagliflozin in the presence of its organic impurities. RSC Advances, 10(12). https://doi.org/10.1039/c9ra08442h
21. Meunier, V., Bourrié, M., Berger, Y., & Fabre, G. (1995). The human intestinal epithelial cell line Caco-2; pharmacological and pharmacokinetic applications. Cell Biology and Toxicology, 11(3–4), 187–194. https://doi.org/10.1007/BF00756522
22. Moorthy, G. S., Stricker, P. A., & Zuppa, A. F. (2015, July 15). A simple and selective liquid chromatography- tandem mass spectrometry method for determination of ε-aminocaproic acid in human plasma. Journal of Applied Bioanalysis, 1(3), 99–107. https://doi.org/10.17145/jab.15.016
23. Mukherjee, D., Srinivasan, B., Anbu, J., Azamthulla, M., Teja, B. V., Ramachandra, S. G., Lakkawar, A. (2019). Pamidronate Functionalized Mucoadhesive Compact for Treatment of Osteoporosis-in Vitro and in Vivo Characterization. Journal of Drug Delivery Science and Technology, 52(June), 915–926. https://doi.org/10.1016/j.jddst.2019.06.001.
24. Ossipov, D. A. (2015). Bisphosphonate-modified biomaterials for drug delivery and bone tissue engineering. Expert Opinion on Drug Delivery, 12(9), 1443–1458. https://doi.org/10.1517/17425247.2015.1021679
25. Pandit, J., Chaudhary, N., Emad, N. A., Ahmad, S., Solanki, P., Aqil, M., & Sultana, Y. (2023). Fenofibrate loaded nanofibers based thermo-responsive gel for ocular delivery: Formulation development, characterization and in vitro toxicity study. Journal of Drug Delivery Science and Technology, 89(August), 104935. https://doi.org/10.1016/j.jddst.2023.104935
26. Pankaj, M., Pavitra, K., Mangla, B., & Aggarwal, G. (2022). Formulation development, optimization by Box-Behnken design, and in vitro characterization of Gefitinib phospholipid complex-based nanoemulsion drug delivery system. Journal of Pharmaceutical Innovation. https://doi.org/10.1007/s12247-022-09690-6
27. Rathee, A., Solanki, P., Verma, S., Vohora, D., Ansari, M. J., Aodah, A., Kohli, K., & Sultana, Y. (2023). Simultaneous determination of posaconazole and hemp seed oil in nanomicelles through RP-HPLC via a quality-by-design approach. ACS Omega. https://doi.org/10.1021/acsomega.3c02097.
28. Raza, A., Murtaza, S. H., Hanif, S., Iqbal, J., Ali, I., Aftab, T., Shakir, R., Bedar, R., & Syed, M. A. (2022). Validation of a rapid and economical RP-HPLC method for simultaneous determination of metformin hydrochloride and sitagliptin phosphate monohydrate: Greenness evaluation using AGREE score. Pakistan Journal of Pharmaceutical Sciences, 35(1). https://doi.org/10.36721/PJPS.2022.35.1.REG.015-021.1
29. Reitsma, P. H., Bijvoet, O. L. M., Verlinden-Ooms, H., & van der Wee-Pals, L. J. A. (1980). Kinetic studies of bone and mineral metabolism during treatment with (3-amino-1-hydroxypropylidene)-1,1-bisphosphonate (APD)

in rats. Calcified Tissue International, 32(1), 145–157. https://doi.org/10.1007/BF02408534
30. Samie, M., Bashir, S., Abbas, J., Khan, S., Aman, N., Jan, H., & Muhammad, N. (2018). Design, Formulation and in Vitro Evaluation of Sustained-Release Tablet Formulations of Levosulpiride. Turkish Journal of Pharmaceutical Sciences, 15(3), 309–318. https://doi.org/10.4274/tjps.29200.
31. Segale, L., Giovannelli, L., Foglio Bonda, A., Pattarino, F., & Rinaldi, M. (2020). Effect of Self-Emulsifying Phase Composition on the Characteristics of Venlafaxine Loaded Alginate Beads. Journal of Drug Delivery Science and Technology, 55, 101483. https://doi.org/10.1016/j.jddst.2019.101483.
32. Shah, R., Pathan, A., Vaghela, H., Ameta, S. C., & Parmar, K. (2019). Green Synthesis and Characterization of Copper Nanoparticles Using Mixture (Zingiber Officinale, Piper Nigrum and Piper Longum) Extract and Its Antimicrobial Activity. Chemical Science Transactions https://doi.org/10.7598/cst2019.1517.
33. Singh, V. D., & Solanki, P. (2016). Isolation and standardisation of antioxidant activity of Bhallatak (Semecarpus Anacardium Linn.). World Journal of Pharmacy and Pharmaceutical Sciences, 5(10), 1021–1028. https://doi.org/10.20959/wjpr201610-7145.
34. Solanki, P., Ansari, D., & Sultana, Y. (2022). Nanostructured Carrageenan as Drug Carrier. In Nanoengineering of Biomaterials. https://doi.org/10.1002/9783527832095.ch17.
35. Solanki, P., Ansari, M. D., Alam, M. I., Aqil, M., Ahmad, F. J., & Sultana, Y. (2022). Precision Engineering Designed Phospholipid-Tagged Pamidronate Complex Functionalized SNEDDS for the Treatment of Postmenopausal Osteoporosis. Springer US. https://doi.org/10.1007/s13346-022-01259-7.
36. Solanki, P., Ansari, M. D., Anjali, Khan, I., Jahan, R. N., Nikita, Pandit, J., Aqil, M., Ahmad, F. J., & Sultana, Y. (2021). Repurposing Pentosan Polysulfate Sodium as Hyaluronic Acid Linked Polyion Complex Nanoparticles for the Management of Osteoarthritis: A Potential Approach. Medical Hypotheses, 157. https://doi.org/10.1016/j.mehy.2021.110713.
37. Solanki, P., Ansari, M. D., Anjali, Khan, I., Jahan, R. N., Nikita, Pandit, J., Aqil, M., Ahmad, F. J., & Sultana, Y. (2021). Repurposing pentosan polysulfate sodium as hyaluronic acid linked polyion complex nanoparticles for the management of osteoarthritis: A potential approach. Medical Hypotheses, 157. https://doi.org/10.1016/j.mehy.2021.110713.
38. Solanki, P., Ansari, M. D., Aqil, M., Ahmad, F. J., & Sultana, Y. (2022). Formulation and Development of Pam-PLc Complex Loaded Self Nano-Emulsifying Drug Delivery System (SNEDDS) for the Treatment of Osteoporosis. SSRN Electronic Journal. https://doi.org/10.2139/ssrn.4004050.
39. Solanki, P., Kumar, A., Garg, A., Sharma, P., & Singh, S. (2012). Designing & development of spherical agglomerates of ibuprofen-paracetamol blend for improved tableting and dissolution. International Journal of Therapeutic Applications, 8, 8–13.
40. Solanki, P., Patel, P. K., & Garg, B. (2013). Formulation Development and Evaluation of Mucoadhesive Buccal Patches of Metoprolol Tartrate. International Journal of Biological and Pharmaceutical Research, 4(12), 1108–1112.
41. Solanki, P., Singh, R., & Singh, V. (2012). Study of complexation of satranidazole with β-cyclodextrin and its effect on solubility and antimicrobial activity. Journal of Drug Delivery Science and Technology, 22(4), 331–337.
42. Solanki, P., Sultana, Y., & Singh, S. (2021). Traditional Medicine: Exploring Their Potential in Overcoming Multi-Drug Resistance. Strategies to Overcome Superbug Invasions: Emerging Research Opportunities, 118–129. https://doi.org/10.4018/978-1-7998-0307-2.ch006.
43. Song, Z., Li, S., Guan, Y., Wang, S., Wang, Y., Yang, G., Zhang, X., Li, J., Song, W., Zhou, C., & Chen, L. (2020). Facile synthesis of zirconia-coated mesoporous silica particles by hydrothermal strategy under low potential of hydrogen conditions and functionalization with dodecylphosphonic acid for high-performance liquid chromatography. Journal of Chromatography A, 1612. https://doi.org/10.1016/j.chroma.2019.460659
44. Tiwari, R., Kumar, A., Solanki, P., Dhobi, M., Sundaresan, V., Kalaiselvan, V., & Raghuvanshi, R. S. (2021). Analytical Quality-by-Design (AQbD) guided development of a robust HPLC method for the quantification of plumbagin from Plumbago species. Journal of Liquid Chromatography & Related Technologies. https://doi.org/10.1080/10826076.2021.1973027.
45. Venkatpurwar, V., & Pokharkar, V. (2011). Green Synthesis of Silver Nanoparticles Using Marine Polysaccharide: Study of in-Vitro Antibacterial Activity. Materials Letters, 65(6). https://doi.org/10.1016/j.matlet.2010.12.057.
46. Wang, X. Q., & Zhang, Q. (2012). pH-Sensitive Polymeric Nanoparticles to Improve Oral Bioavailability of Peptide/Protein Drugs and Poorly Water-Soluble Drugs. European Journal of Pharmaceutics and Biopharmaceutics. https://doi.org/10.1016/j.ejpb.2012.07.014.

47. Yin, Q., Tang, L., Cai, K., Tong, R., Sternberg, R., Yang, X., Dobrucki, L. W., Borst, L. B., Kamstock, D., Song, Z., Helferich, W. G., Cheng, J., & Fan, T. M. (2016). Pamidronate functionalized nanoconjugates for targeted therapy of focal skeletal malignant osteolysis. Proceedings of the National Academy of Sciences of the United States of America, 113(32), E4601–E4609. https://doi.org/10.1073/pnas.1603316113
48. Zakir, F., Ahmad, A., Farooq, U., Mirza, M. A., Tripathi, A., Singh, D., Shakeel, F., Mohapatra, S., Ahmad, F. J., & Kohli, K. (2020). Design and development of a commercially viable in situ nanoemulgel for the treatment of postmenopausal osteoporosis. Nanomedicine, 15(12),1167–1187. https://doi.org/10.2217/nnm-2020-0079